Structure and opto-electronic properties of MgO nanocrystals calculated by GGA approximation

M. Myvizhi[a], K.V. Satheesh Kumar[b], P. R. Kavitha[c], P. Selvakumar[d*]
[a]*Department of Mathematics, KPR Institute of Engineering and Technology, Coimbatore, 641407, Tamilnadu, India*
[b]*Department of Mechanical Engineering, Kongu Engineering College, Perundurai, Erode, 638060, Tamilnadu, India*
[c]*Department of Mathematics, KG College of Arts and Science, Coimbatore, 641035, Tamilnadu, India*
[d]*Department of Humanities and Sciences, Gokaraju Rangaraju Institute of Engineering and Technology, Hyderabad, 500090, Telangana, India*

This study uses the CASTEP code and the density functional theory (DFT) to look into the structure, electrical properties, and optical properties of MgO. The generalised gradient approximation (GGA-PW91 approximation) was used to measure both the energy of the band gap and the energy of the exchange-correlation. This computation was done based on the cubic MgO crystal structure, which has a space group of Fm-3m and a 3x3x3 supercell. In structural optimization, the results that are expected for the lattice constant and the bulk modulus elastic constant are very close to known experiments and theories. The anticipated direct band gap of 4.283eV at the G point is in excellent agreement with the results of the tests. Also, the total (DOS) and partial (PDOS) densities of states have been measured, and the results of the absorption coefficient have been looked at in terms of the different energies of the phonons that hit the material.

(Received October 14, 2022; Accepted May 4, 2023)

Keywords: CASTEP, GGA approximation, MgO, Structure, Opto-electronic properties

1. Introduction

Metal oxides are fundamental functional materials having many uses in chemistry, physics, and materials science[1]. Due to their simple and controlled synthesis, they are often used for photocatalytic applications[2], biomedical engineering[3], and sensors[4]. The size and surface morphology of metal oxides are influenced by the synthesis technique, pH, temperature, and annealing time and may thus be manipulated throughout the growth process[5]. Magnesium oxide (MgO), an insulator with a broad bandgap, has prospective uses in electronics owing to its alluring characteristics, such as cheap cost, non-toxicity, high-temperature resistance, optical transparency, and abundant earthy availability. Due to their distinct and often modifiable features, metal oxide nanocrystal powders have several uses[6]. Understanding photoexcited processes has been the subject of much study on such nano powders. The characteristics of nanoparticles vary from those of bulk materials. Due to their unique hydrophobic, photocatalytic, and stable properties, metal oxide nanoparticles are used by the majority of researchers[7]. Researchers all around the globe have been drawn to MgO nanoparticles due to their enormous bandgap and low production cost. MgO is an insulator with a bandgap of 7eV and a significant bandgap. The lower bandgap of MgO nanoparticles is responsible for their higher reactivity. On MgO nanocrystals, several theoretical and experimental research have been conducted too far[8]. Solid-state density functional theory (DFT) is a powerful tool for estimating the optical and electrical characteristics of molecules[9].

Few approaches exist for determining electrical and optical characteristics, such as Local Density Approximation (LDA) and Generalized Gradient Approximation (GGA) calculations based on basic principles[10]. In the case of transition metal oxides, however, these techniques

* Corresponding author: selvakumarpresec@gmail.com
https://doi.org/10.15251/JOR.2023.193.265

significantly underestimate the bandgap. The GGA functional is often regarded as dependable. It does not affect the structure's bandgap pattern[11]. This study used the first principle functional density theory (DFT) to perform a detailed calculation of the electronic properties of the MgO compound. After calculating the structure and optoelectronic properties comparing it with experimental results, then determined and analysed the state densities characteristics (total and partial).

2. Method of calculation

Theoretical investigations conducted in Cambridge flat-wave voltage false total energy (CASTEP) using DFT[12]. The ultra-soft pseudo potential is utilised to characterise the electron-ion interaction. MgO is a member of the Fm-3m space group with a face-centered cubic (FCC) structure and lattice parameters of a = 4.2168Å. The theoretical model for the crystal structure of undoped MgO is seen in Fig.1. Green symbolises Mg atoms, whereas red indicates O atoms. The calculations are done using an ultra-soft pseudo potential approach using Mg($2p^6 3s^2$) and O electronic valence configurations ($2s^2 2p^4$). For the exchange connection between electrons and the cut off energy of a 400eV plane wave, the GGA -PW91 approximation was used[13]. Monk horst-Pack (MP) k-meshes of 3X3X3 face-centered cubic structures are used to guarantee overall energy convergence within 5 X 10^{-6} eV/atom.

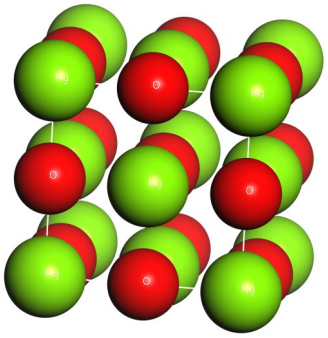

Fig 1. Cubic MgO nanocrystal structure

3. Result and Discussion

3.1. Structure

In order to create a stable structure, the MgO nanocrystal's smallest shape was optimised on the basis of the unit cell. Bulk MgO was found to have an initial lattice parameter (cubic, a = b = c) of 4.216Å[14]. This was obtained by creating a cubic structure in Materials Studio Visualizer using space group 225 (Fm-3m) (Fig.1). Wyckoff position 4a (0,0,0) was held by Mg atoms, whereas 4b (0.5,0.5,0.5) was occupied by O atoms. Valence electrons were in O (2s, 2p) and Mg (2p, 3s) atoms. The MgO nanocrystal was then completely relaxed to a0 = 4.299 Å, and the Mg–Mg and Mg–O bond lengths are 3.040 Å and 2.150 Å, respectively.

3.2. Elastic constants

C11, C12, and C44 are the three free elastic constants that define the mechanical stability of MgO. Typically, they are deduced by calculating the crystal's total energy, which indicates its elastic properties, and the stability condition of the cubic crystal is provided by

$$C_{11} - C_{12} > 0, C_{11} + 2C_{12} > 0, C_{44} > 0 \quad (1)$$

C11 > |C12| is the first condition, whereas C11 > 0 is indicated by the first and second conditions. These requirements are satisfied by the GGA-measured constants of elasticity. Therefore, the MgO

structure is mechanically stable. In the study of the results produced by the two approximations, the sequence C11 > C44 > C12 is seen, which is consistent with the experimental and theoretical results[15]. The findings of elastic constant indicate A of MgO (anisotropy coefficient) was found via the expression, which represents a crystal anisotropy calculation.

$$A = \frac{C_{11}-C_{12}}{2C_{44}} \quad (2)$$

A totally isotropic material has an A value of 1, hence the anisotropy value of a crystal might be less than or greater than unity. The measured A value for the GGA was 0.63. MgO is thus perfectly anisotropic in terms of elasticity, as shown by[16].

3.3. Density of state and electronic band structure

Fig.2 shows the band structure of a MgO crystal. The equilibrium bandgap of MgO was predicted to be 4.180eV as an insulator with a large direct bandgap. The CBM and VBM occupy identical k-vector locations inside the Brillouin zone. Due to covalent bonding, the valence band is completely filled with electrons. They must thus attain energy equivalent to the bandgap in order to enter the conduction band and attain conductivity. The measured bandgap value is quite similar to a prior GGA-based theoretical analysis with a value of 4.283eV. Mg has the electrical configuration $1s^2\ 2s^2\ 2p^6\ 3s^2$, whereas O has just $1s^2\ 2s^2\ 2p^4$.

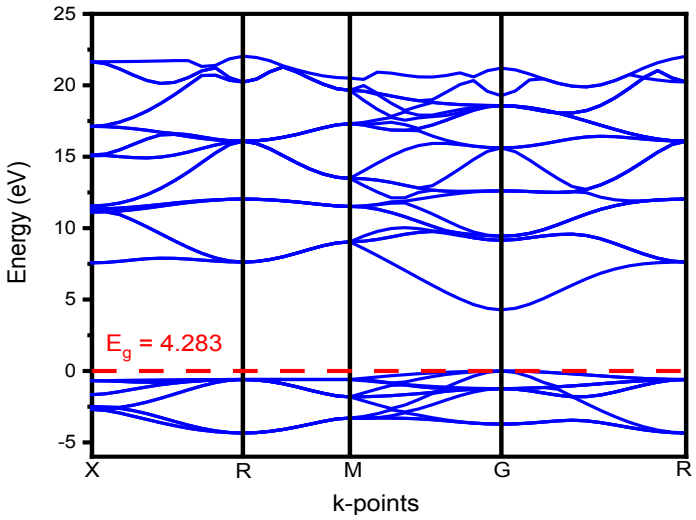

Fig. 2. The band gap structure of MgO (electronic) using GGA approximation.

In spite of this, after magnesium is linked to oxygen, the electronic configuration of Mg^{2+} and O^{2-} changes to the one (Fig. 3), which means that all of the 2p orbitals are paired with one another. MgO is a very stable molecule because the both Mg^{2+} and O^{2-} electron configurations contain 2p orbitals that are completely filled.

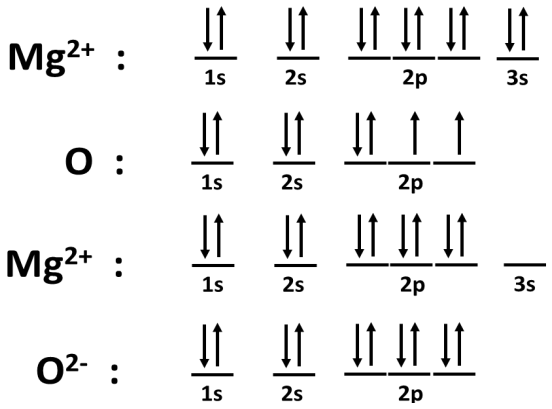

Fig. 3. Electron configuration of Mg and O atoms and of MgO.

Fig.4 depicts TDOS (total density of states) for MgO and PDOS (partial density of states) for the Mg and O atoms individually. Mg atoms 3p-orbital and O atoms 2p-orbital mostly occupy the lowest conduction band and maximum valence band, respectively.

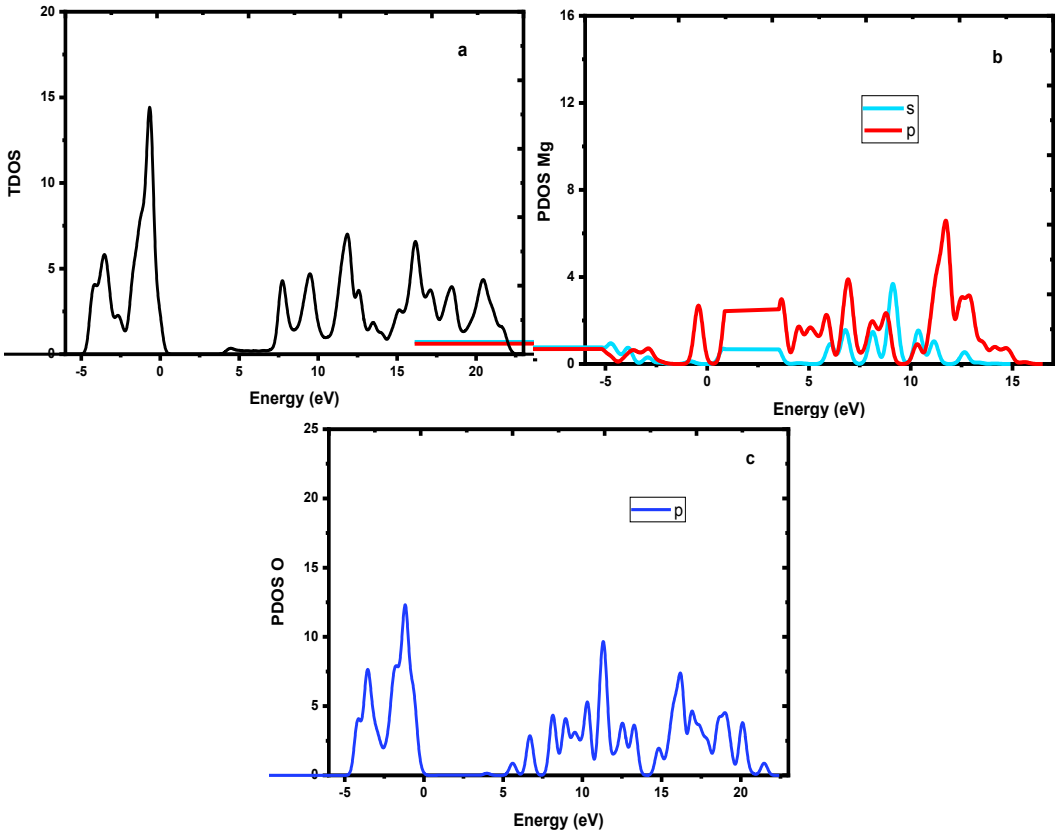

Fig. 4. (a) TDOS (Total density of states) by GGA; (b) & (c) PDOS (Partial density of states) for Mg and O by GGA.

3.4. Optical properties

Important physical characteristics are required for research and instrumentation applications in order to analyse the interactions between incoming photons and the compound MgO based on its optical property[17]. The dielectric function characterises the optical response of a material to various photon energies. The real factor ε1(ω) may be determined using the Kramer-

Kronig relationship, which relates ε1(ω) and ε2(ω). From the elements of the matrix in the wave function for occupied and unoccupied states, the function ε2(ω) may be determined. Further optical characteristics, (K(ω)), (R(ω)), (n(ω)), Extinction coefficient, the Reflectance, the Refractive index and the Absorption coefficient are derived from ε1(ω) and ε2(ω). The function for the buffer is stated as:

$$\varepsilon(\omega) = \varepsilon_1(\omega) + \mathrm{i}\varepsilon_2 \tag{3}$$

$$\varepsilon_1(\omega) = 1 + \frac{2}{\pi}\mathrm{p}\int_0^{\infty} \frac{\omega'\varepsilon_2(\omega)}{\omega'^2-\omega^2}\mathrm{d}\omega' \tag{4}$$

$$\varepsilon_2(\omega) = -\frac{2\omega}{\pi}\mathrm{p}\frac{\varepsilon_1(\omega')}{\omega'^2-\omega^2}\mathrm{d}\omega' \tag{5}$$

$$\alpha(\omega) = \sqrt{2}\left[\sqrt{\varepsilon_1^2(\omega)+\varepsilon_2^2(\omega)} - \varepsilon_1(\omega)\right]^{\frac{1}{2}} \tag{6}$$

$$\mathrm{R}(\omega) = \frac{|\sqrt{\varepsilon(\omega)}-1|^2}{|\sqrt{\varepsilon(\omega)}+1|^2} \tag{7}$$

$$\mathrm{n}(\omega) = \frac{1}{\sqrt{2}}\left[(\varepsilon_1^2(\omega)+\varepsilon_2^2(\omega))^{\frac{1}{2}} + \varepsilon_1(\omega)\right]^{\frac{1}{2}} \tag{8}$$

$$K(\omega) = \frac{1}{\sqrt{2}}\left[(\varepsilon_1^2(\omega)+\varepsilon_2^2(\omega))^{\frac{1}{2}} - \varepsilon_1(\omega)\right]^{\frac{1}{2}} \tag{9}$$

where p – Integral value of the Cauchy principal[18], ε1(ω) reflects material's storage energy capability, and ε2(ω) reveals the absorption behaviour and structure of electronic band [19]. Fig.5a & 5b displays parts of the imaginary and real functions of isolation for MgO in the 0-25eV photon energy range. The distinct peaks of ε2(ω) exhibited in Fig.5a resulted from the transmission of electrons from valence to the conduction bands occurs directly via symmetric lines (Γ- F – Q – Z – Γ). The energy of threshold ε2(ω) for MgO (3.55eV), which corresponds to the electrons transitions from VB_{Max} to CB_{Min} at high symmetry points and represents fundamental absorption edge of solid solutions (bandgap). Here ε2(ω) grows with increasing energy and exhibits prominent absorption peaks in the 11.6–12.7eV energy range. The greatest values of ε2(ω) in Table.1 high energy range indicate that MgO behaves like energy filter function under UV (Ultraviolet) spectrum. Figure 5b depicts the difference between the real component ε1(ω) of the dielectric function of MgO and photon energy. Fig.5c, the MgO absorption (ω) coefficient at photon energy is shown.

Table 1. Calculated optical properties for MgO.

Optical Properties	ε1(0)	ε1(ω) max	ε2(ω) max	R(0)	n(ω)	k(ω)
MgO	3.55	7.15	12.6	0.89	1.88	11.7

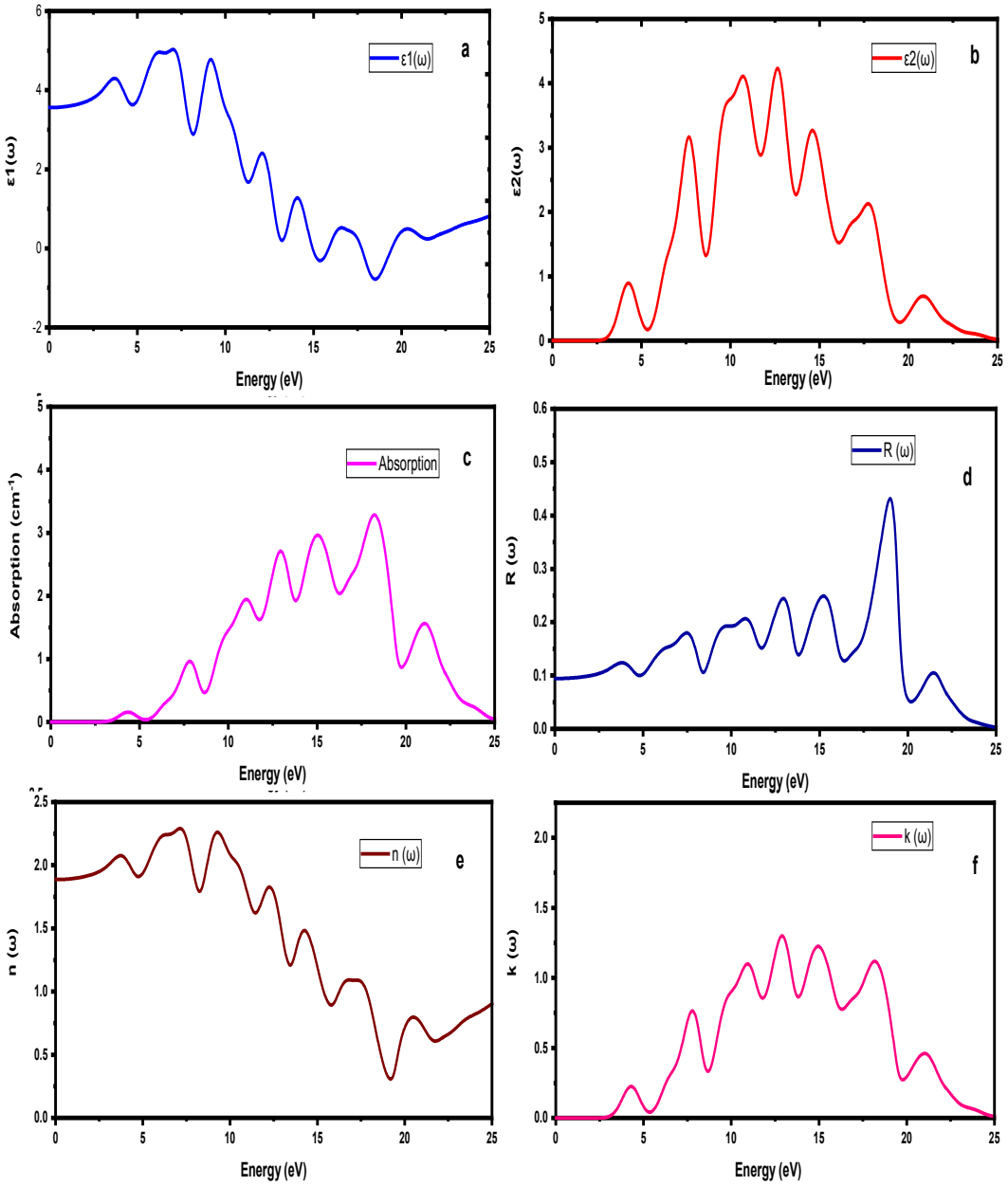

Fig. 5. Displays static optical characteristics ε1(ω), ε2(ω), Absorption, (R(ω)), n(ω) and k(ω) for MgO.

Electron transport between the valence O_{2P} orbital to the conduction Mg_{3S} orbital which is responsible for MgO's optical absorption in the UV light range. At 4.282eV, the intensities of the significant MgO adsorption peaks are measured. Fig.5d depicts the reflectance of MgO in relation to photon energy. Calculated static reflectivity values for MgO are 0.89. Reflectivity of MgO rises straight with energy from photon till it spreads its extreme value between 11.8 and 18.7eV. The R (ω) value of a substance indicates its surface roughness. According to Fig.5e, displays a correlation among the path of the refractive index (ω) and the path of ε1(ω) with the energy photon. The value of n(ω) was constant for MgO (1.88). In Fig.5f, the extinction coefficient of MgO was plotted versus the photon energy. The (ω) values for MgO grow progressively with increasing energy of photon and obtains to maximum values from 11.7eV to 13.8eV in the region, indicating absorption maximum.

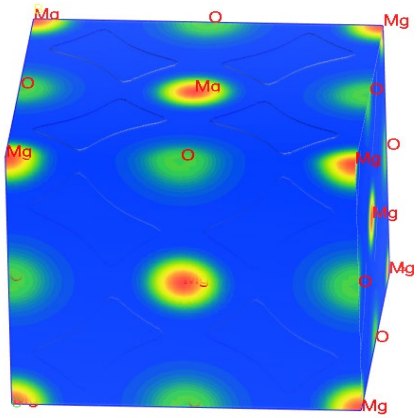

Fig. 6. Charge density distribution map of MgO (110) planes using GGA.

3.5. Charge density distribution

Fig.6 depicts the distributions of charge density of valence electron (e/A^3) inside the 3D 110 planes derived from the GGA analysis of the nature of MgO atomic bonds. The density of electrons is shown by the colour scale maps. The shades of blue and red represent the highest and lowest densities of electron, respectively. The distributions of density of charge in the preceding maps reveal that around the atomic O species is substantially cubic due to the surrounding charge distribution of Mg atoms. This is evidence for covalent bonding. Meanwhile the O atoms charge is greater compared to that of Mg atoms, due to ionic contribution. The distribution maps of charge density, MgO compounds exhibit clear indications of covalent interaction between Mg-Mg, Mg-O, and O-O atoms. These results validate the Mullikan bond population studies for 3D and flat structures (110). The MgO maps of charge density reveal that the Mg atom has higher densities of electron than the O atom. Mg and O atoms lack electrons and have spherical charge distributions in MgO. These properties contribute ionically to the overall bonding.

3.6. Mulliken Bond population studies

Mulliken bond population studies (MBPS) was used to further investigate the nature of MgO bonding molecule[20] and the outcomes are shown in Tables 2 and 3. From MBPS, each Mg atom in MgO transfers 1.21 electrons to each O atom. Typically, the Mulliken charge and population overlap measures relative strength of chemical bonds between atoms. In addition, employed the effective valence to determine the dominance of bonding (covalent or ionic)[21]. MgO is a perfect ionic bond with a valence of zero, while the analogous covalent bond has a larger valence.

Table 2. Orbital electron charges, Overall charge and Mulliken charge(e) of MgO by GGA.

Species	s	p	d	f	Over all	Mullikan Charge (e)
Mg	1.95	5.26	0	0	7.21	1.21
O	0.59	6.20	0	0	6.79	-1.21

Table.2 displays the total and effective valence charges of the MgO species. The transfer charge between O and Mg are approximately (-1.21e, 1.21e). Therefore, covalent and ionic characteristics coexist with MgO's bonding behaviour. Table.3 displays the calculated results of Mulliken bond populations and bond lengths in MgO using GGA functions. Negative (antibonding) and positive bond (bonding) states population numbers respectively. MgO has a bond length (Mulliken) of 2.147Å and for O-O was 3.036Å. These findings confirm the aforementioned estimates of the states' electronic structures and densities.

Table 3. Estimated bond population overlaps and bond lengths (Mulliken) for MgO by GGA.

Bond	Population	Lengths (Å)
Mg-O	0.56	2.1472
O-O	0.29	3.0365

4. Conclusion

Using CASTEP first principle calculations, the current work explored the structure and optoelectronic characteristics of MgO. The findings derived using GGA are congruent with experimental evidence and existing theory. The elastic constants are initially predicted using the GGA technique, and calculations demonstrate that MgO exhibits elastic anisotropy and elastic stability at room temperature. The band structure and DOS data indicate that band gap of semiconductor MgO is a direct. The band gap energy (4.283eV), which is both lower than the experimental band gap and an underestimate. Based on estimates of the DOS, PDOS and bond population, the chemical bonding in MgO was determined to be both ionic and covalent. The estimated optical absorption is in excellent agreement with the experimentally determined value.

References

[1] W. Chaikittisilp, Y. Yamauchi, K. Ariga, Adv. Mater. 34, 2107212 (2022); https://doi.org/10.1002/adma.202107212
[2] M.S.S. Danish, L.L. Estrella, I.M.A. Alemaida, A. Lisin, N. Moiseev, M. Ahmadi, M. Nazari, M. Wali, H. Zaheb, T. Senjyu, Metals. 11 (1), 80 (2021); https://doi.org/10.3390/met11010080
[3] X. Yang, E. Chung, I. Johnston, G. Ren, Y.-K. Cheong, Appl. Sci. 11(10), 4520 (2021); https://doi.org/10.3390/app11104520
[4] S. Yang, G. Lei, H. Xu, Z. Lan, Z. Wang, H. Gu, Nanomaterials. 11(4), 1026 (2021); https://doi.org/10.3390/nano11041026
[5] S. Arya, P. Mahajan, S. Mahajan, A. Khosla, R. Datt, V. Gupta, S.-J. Young, S.K. Oruganti, ECS J. Solid State Sci. Technol. 10, 023002 (2021); https://doi.org/10.1149/2162-8777/abe095
[6] T. Naseem, T. Durrani, Environ. Chem. Ecotoxicol. 3, 59 (2021); https://doi.org/10.1016/j.enceco.2020.12.001
[7] K.R. Singh, V. Nayak, J. Singh, A.K. Singh, R.P. Singh, RSC Adv. 11, 24722 (2021); https://doi.org/10.1039/D1RA04273D
[8] R. Kant, A.K. Singh, A. Arora, Vacuum. 189, 110247 (2021); https://doi.org/10.1016/j.vacuum.2021.110247
[9] Z. Tao, X. Xu, L. Bi, Electrochem. Commun. 129, 107072 (2021); https://doi.org/10.1016/j.elecom.2021.107072
[10] F. Saadaoui, M. Zemouli, F.-Z. Driss-Khodja, T. Djaafri, M. Driss-Khodja, 1st Int. Conf. Comput. Appl. Phys., 115 (2022)
[11] K. Brown, Y. Maimaiti, K. Trepte, T. Bligaard, J. Voss, J. Comput. Chem. 42, 2004 (2021); https://doi.org/10.1002/jcc.26732
[12] S.-R.G. Christopoulos, K.A. Papadopoulou, A. Konios, D. Parfitt, Comput. Mater. Sci. 202 110976 (2022); https://doi.org/10.1016/j.commatsci.2021.110976
[13] D. Hong, W. Zeng, F.-S. Liu, B. Tang, Q.-J. Liu, Mater. Chem. Phys. 259, 124029 (2021); https://doi.org/10.1016/j.matchemphys.2020.124029
[14] Z. Liu, X. He, Z. Mei, H. Liang, L. Gu, X. Duan, X. Du, J. Phys. Appl. Phys. 47, 105303 (2014); https://doi.org/10.1088/0022-3727/47/10/105303
[15] G. Sha, Insight-Non-Destr. Test. Cond. Monit. 60(4), 190 (2018); https://doi.org/10.1784/insi.2018.60.4.190
[16] M.L. Dos Reis, P. Carrez, P. Cordier, Phys. Rev. Mater. 5, 063602 (2021); https://doi.org/10.1103/PhysRevMaterials.5.063602
[17] L.E. Low, S.P. Siva, Y.K. Ho, E.S. Chan, B.T. Tey, Adv. Colloid Interface Sci. 277, 102117

(2020); https://doi.org/10.1016/j.cis.2020.102117
[18] E. Haque, M.A. Hossain, Mater. Sci. Semicond. Process. 83, 192 (2018); https://doi.org/10.1016/j.rinp.2018.08.051
[19] M. Nesa, M.A. Momin, M. Sharmin, A.H. Bhuiyan, Chem. Phys. 528, 110536 (2020); https://doi.org/10.1016/j.chemphys.2019.110536
[20] S. Merazka, L. Hammoudi, M. Kars, M. Sidoumou, T. Roisnel, J. Mod. Mater. 8, 3 (2021); https://doi.org/10.21467/jmm.8.1.3-11
[21] D.M. Hoat, V. Van On, D.K. Nguyen, M. Naseri, R. Ponce-Pérez, T.V. Vu, J.F. Rivas-Silva, N.N. Hieu, G.H. Cocoletzi, RSC Adv. 10, 40411 (2020); https://doi.org/10.1039/D0RA05030J